Local electronic structure in a LiAlO$_2$ single crystal studied with ^{7}Li NMR spectroscopy and comparison with quantum chemical calculations

Sylvio Indris* and Paul Heitjans†

Institut für Physikalische Chemie und Elektrochemie, Leibniz Universität Hannover, Callinstraße 3-3A, D-30167 Hannover, Germany

Reinhard Uecker

Institut für Kristallzüchtung, Max-Born-Straße 2, D-12489 Berlin, Germany

Thomas Bredow‡

Theoretische Chemie, Leibniz Universität Hannover, Am Kleinen Felde 30, D-30167 Hannover, Germany

The local electronic structure of a γ-LiAlO$_2$ single crystal was investigated with ^{7}Li nuclear magnetic resonance measurements. We observed different sets of spectra which originate from the four crystallographically equivalent but magnetically inequivalent Li sites per unit cell. We find a coupling constant e^2qQ/h $=115.1\pm0.6$ kHz and an asymmetry parameter $\eta=0.69\pm0.01$. The directions of the principal axes of the electric field gradient tensor at the sites of the Li nuclei have also been determined. We compared these experimental results with quantum chemical calculations at density-functional level and found good agreement.

I. INTRODUCTION

γ-LiAlO$_2$ crystallizes in the tetragonal space group $P4_12_12$. A unit cell of this crystal contains four formula units and has lattice parameters $a=5.1687\pm0.0005$ Å and $c=6.2679\pm0.0006$ Å.[1] There are four chemically equivalent but magnetically inequivalent sites for the Li atoms as well as for the Al atoms. The Li as well as the Al atoms are located inside oxygen tetrahedra. Each LiO$_4$ tetrahedron shares a common edge with an AlO$_4$ tetrahedron. These pairs of LiO$_4$-AlO$_4$ tetrahedra are connected via common oxygen corners and form a three-dimensional regular lattice, see Fig. 1. The positions of the atoms in the unit cell are given in Table I.[1]

LiAlO$_2$ has many different applications. It is used as substrate material for epitaxial growth of III-V semiconductors like GaN,[2] as coating in Li electrodes[3] and as additive in composite Li electrolytes.[4] LiAlO$_2$ is also considered as candidate material for tritium breeder or fusion reactors.[5] First NMR measurements were performed on powder samples to determine structure-dependent parameters like electric field gradients and chemical shifts at the Al sites.[6]

For the analysis of the ^{7}Li NMR spectra and their angular dependencies, the Hamiltonian for an $I=3/2$ nucleus system is

$$\hat{H} = \hat{H}_Z + \hat{H}_Q, \tag{1}$$

where $\hat{H}_Z$ is the nuclear Zeeman term and $\hat{H}_Q$ describes the nuclear quadrupole interaction. $\hat{H}_Q$ is expressed as[7–9]

$$\hat{H}_Q = \frac{eQ}{2I(2I-1)h}\hat{\boldsymbol{I}} \cdot \mathbf{V} \cdot \hat{\boldsymbol{I}}, \tag{2}$$

where $\mathbf{V}$ is the electric field gradient tensor at the site of the nucleus, $\hat{\boldsymbol{I}}$ is the nuclear spin vector, e is the elementary charge, h is Planck's constant, and Q the nuclear quadrupole moment.

II. SAMPLE PREPARATION

LiAlO$_2$ single crystals were grown using the Czochralski technique with radio frequency (rf) induction heating. The main problem of the growth of these crystals is the strong selective evaporation of Li$_2$O from the melt as well as from the crystal. Its suppression required particular temperature gradients extremely different from the standard ones for oxides. The found conditions allow the growth of LiAlO$_2$ crystals up to 2 in. diameter and 80 mm length with good perfection. The starting melt was prepared from predried ^{7}Li$_2$CO$_3$ (99.99%) and Al$_2$O$_3$ (99.99%) powders which were mixed in the stoichiometric ratio and sintered subsequently. Due to the high melting temperature of about 2000 K both the crucible and the active afterheater were made of iridium. The pulling rate was 1.5 mm h^{-1} and the rotation rate was 10 min^{-1}. Flowing argon was used as the growth atmosphere. The crystals were pulled along the [110] orientation.
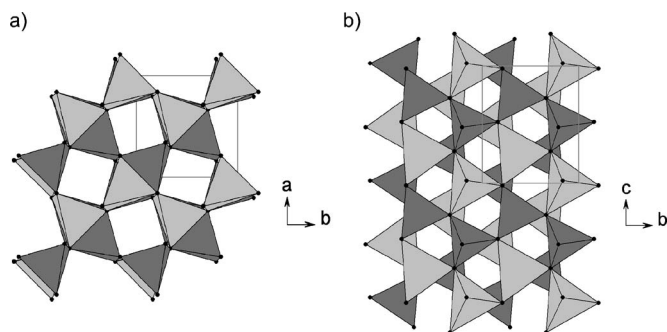

FIG. 1. Tetragonal crystal structure of γ-LiAlO$_2$ (space group $P4_12_12$). The Li atoms as well as the Al atoms are located inside oxygen tetrahedra (light gray and dark gray tetrahedra, respectively) forming a three-dimensional network. a) view along the c axis. b) view along the a axis.

TABLE I. Positions of the atoms in the tetragonal unit cell ($a=5.1687\pm0.0005$ Å and $c=6.2679\pm0.0006$ Å).[1] All coordinates are given in Å.

Atom	Measured (Ref. [1])			Calculated (present work)		
	x	y	z	x	y	z
Li(1)	4.200	4.200	0.000	4.235	4.235	0.000
Li(2)	3.553	1.616	1.567	3.579	1.630	1.581
Li(3)	0.969	0.969	3.134	0.974	0.974	3.163
Li(4)	1.616	3.553	4.701	1.630	3.579	4.744
Al(1)	0.909	0.909	0.000	0.917	0.917	0.000
Al(2)	1.675	3.494	1.567	1.688	3.521	1.581
Al(3)	4.260	4.260	3.134	4.292	4.292	3.163
Al(4)	3.494	1.675	4.701	3.521	1.688	4.744
O(1)	1.741	1.502	4.841	1.751	1.520	4.883
O(2)	1.082	4.326	0.140	1.085	4.355	0.139
O(3)	3.427	3.667	1.707	3.458	3.689	1.721
O(4)	4.086	0.843	3.274	4.124	0.854	3.302
O(5)	4.326	1.082	6.128	4.355	1.085	6.186
O(6)	0.843	4.086	2.994	0.854	4.124	3.023
O(7)	1.502	1.741	1.427	1.520	1.751	1.442
O(8)	3.667	3.427	4.561	3.689	3.458	4.604

III. EXPERIMENTAL SETUP

Static ^{7}Li NMR line shapes were measured at room temperature on a Bruker MSL 400 spectrometer for different orientations of the single crystal with respect to the magnetic field. The orientation of the single crystal (size: $5\times5\times4$ mm^3) was adjusted via a Teflon carrier inserted in the rf coil of the NMR probe. A solid-echo pulse sequence was used to avoid dead-time effects. Typically 256 scans were acquired with a recycle delay of 100 s.

IV. QUANTUM CHEMICAL CALCULATIONS

Periodic calculations at density-functional level were performed for γ-LiAlO$_2$ using the crystalline-orbital program CRYSTAL03.[10] In CRYSTAL the Bloch functions are constructed from atom-centered Gaussian-type atomic orbitals. In the present calculations all-electron basis sets were employed, in particular, 85-11G* for Al,[11] 8-411G* for O,[12] and 7-11G* for Li. The latter basis has been developed in our previous study of the electric field gradient at the Li position in LiTiS$_2$ (Ref. [13]) where quantitative agreement between calculated and measured field gradients was obtained. The exchange-correlation functional PW91 (Ref. [14]) was used as in the previous study.[13] In a first step, the structural parameters (lattice constants and fractional coordinates of the atoms) were optimized starting from the experimental values.[1] The calculated values of a and c, 5.18 Å and 6.29 Å, respectively, are in good agreement with the measured values, 5.169 Å and 6.268 Å (Table I). Also the deviations for the atomic coordinates (Table I) are less than 0.04 Å, corresponding to relative
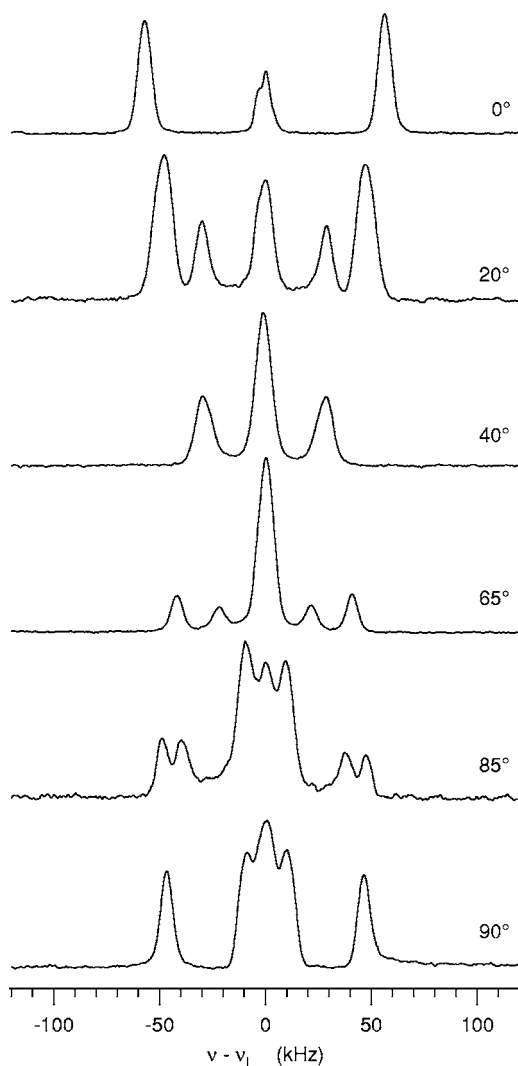

FIG. 2. ^{7}Li NMR spectra of the γ-LiAlO$_2$ single crystal for different orientations of the magnetic field with respect to the crystal structure. The figure shows exemplarily orientations between the [001] direction (0°) and the [110] direction (90°).

errors smaller than 1%. The EFG tensor at the Li positions was calculated for the fully optimized structure. In all calculations the cutoff thresholds for integral calculation were decreased by three orders of magnitude compared to the standard settings of CRYSTAL in order to increase numerical precision. Summation over the reciprocal lattice was performed using the Monkhorst-Pack scheme.[15] 75 special k points were taken into account in the irreducible Brillouin zone.

V. RESULTS

Some ^{7}Li NMR spectra of the γ-LiAlO$_2$ single crystal are shown in Fig. 2. For the acquisition of the spectra in this figure, the single crystal was turned that way that the magnetic field with respect to the crystal structure is moved from the [001] direction (0°) to the [110] direction (90°). According to the nuclear spin of ^{7}Li ($I=3/2$) different sets of triplet
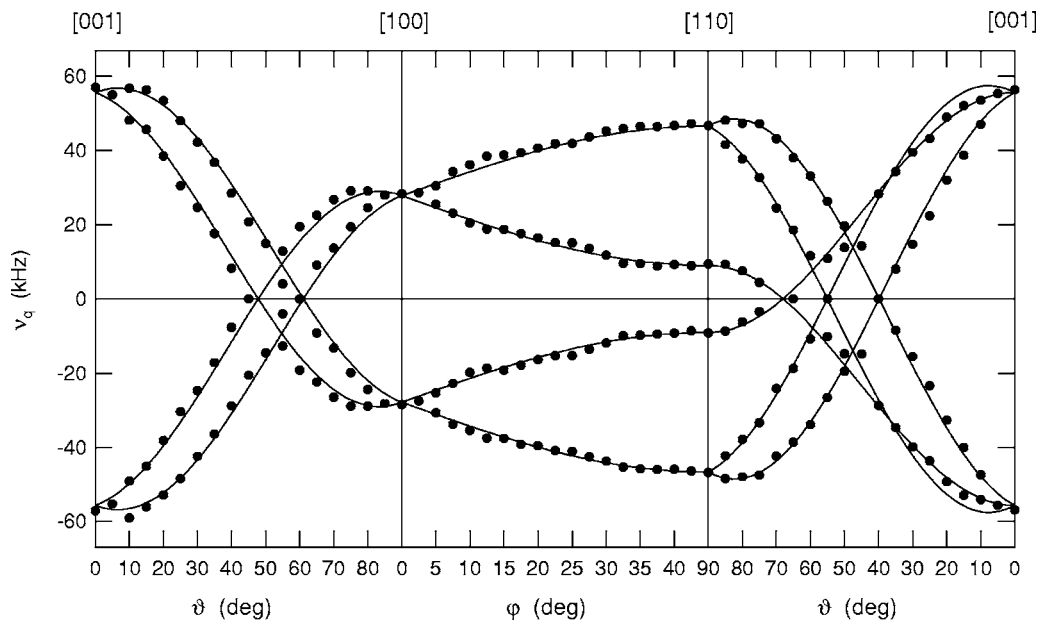
FIG. 3. Resonance frequencies ν_q of the quadrupole satellites in the ^{7}Li NMR spectra of a LiAlO$_2$ single crystal for different orientations of the magnetic field with respect to the crystal structure. ϑ and φ denote the tilt angles of the magnetic field with respect to the main crystal axes which are given on the upper abscissa. The full circles represent experimental data. The solid lines show the results of a three-parameter fit according to Eqs. (2) and (3) yielding the eigenvalues and the eigenvectors of the electric field gradient tensor.

patterns are visible. The central line, belonging to the transition $(|+1/2\rangle \leftrightarrow |-1/2\rangle)$, which is not affected by interaction of the quadrupole moment of the ^{7}Li nucleus with electric field gradients at the site of the nucleus, is located at the larmor frequency ν_L for all triplets. Sharp quadrupole satellites, belonging to the transitions $(|+3/2\rangle \leftrightarrow |+1/2\rangle)$ and $(|-1/2\rangle \leftrightarrow |-3/2\rangle)$, are located at $\nu_L \pm \nu_q$ where $\nu_q = eQV_B/2h$ is the quadrupole coupling frequency. V_B is the electric field gradient in the direction of the magnetic field. The quadrupole moment of the ^{7}Li nucleus is $Q(^7\text{Li})$ $= -4.01 \times 10^{-30}$ m^2.[16] In the spectra more than one satellite pair, i.e., more than one triplet pattern, is visible. This is due to the fact that the four Li atoms per unit cell are not equivalent any more in the presence of the magnetic field which reduces the overall symmetry of the unit cell (except for the case where the magnetic field is aligned parallel to the main symmetry axis of the crystal structure, which is the c axis in this case).

Taking into account that the EFG matrix is symmetric and traceless, i. e., $V_{ij} = V_{ji}$ and $V_{xx} + V_{yy} + V_{zz} = 0$, the tensor has, in general, only five independent elements. Furthermore, since the structure of γ-LiAlO$_2$ is tetragonal and the four crystallographically equivalent Li sites are arranged around a fourfold screw axis, V_{xz} and V_{yz} differ only by their sign and $V_{xx} = V_{yy}$. Therefore, three independent parameters are sufficient to describe the electric field gradient tensor completely. We used a matrix of the form

$$\mathbf{V} = \begin{pmatrix} V_{xx} & V_{xy} & V_{xz} \\ V_{yx} & V_{yy} & V_{yz} \\ V_{zx} & V_{zy} & V_{zz} \end{pmatrix} = \begin{pmatrix} A & B & C \\ B & A & -C \\ C & -C & -2A \end{pmatrix} \quad (3)$$

to describe the EFG at the site of the Li(1) atom. x, y, and z belong to the main axes of the crystal structure, and A, B, and C are the three fit parameters.

The EFG tensors for the other Li atoms in the unit cell, being crystallographically equivalent to Li(1), can be derived from this, according to the symmetry of the crystal structure, by successive stepwise rotation of the EFG tensor around the z axis by 90°. Therefore only three parameters have been used to fit all branches in Fig. 3 simultaneously.

The three-parameter fit gives for the EFG tensor elements at the Li(1) position:

$$V_{xx} = V_{yy} = (0.574 \pm 0.002) \text{ V/Å}^2,$$

$$V_{xy} = (-0.388 \pm 0.003) \text{ V/Å}^2,$$

$$V_{xz} = -V_{yz} = (0.203 \pm 0.003) \text{ V/Å}^2. \quad (4)$$

From this we can extract the eigenvalues

$$V_{A,\text{exp}} = (-1.187 \pm 0.006) \text{ V/Å}^2,$$

$$V_{B,\text{exp}} = (0.186 \pm 0.007) \text{ V/Å}^2,$$

$$V_{C,\text{exp}} = (1.001 \pm 0.009) \text{ V/Å}^2, \quad (5)$$

and the corresponding eigenvectors (expressed in the Cartesian coordinates of the crystal structure)

$$\vec{e}_{A,\text{exp}} = \begin{pmatrix} -0.094 \\ 0.094 \\ 0.991 \end{pmatrix}$$

$$\vec{e}_{B,\text{exp}} = \begin{pmatrix} 0.707 \\ 0.707 \\ 0 \end{pmatrix}$$
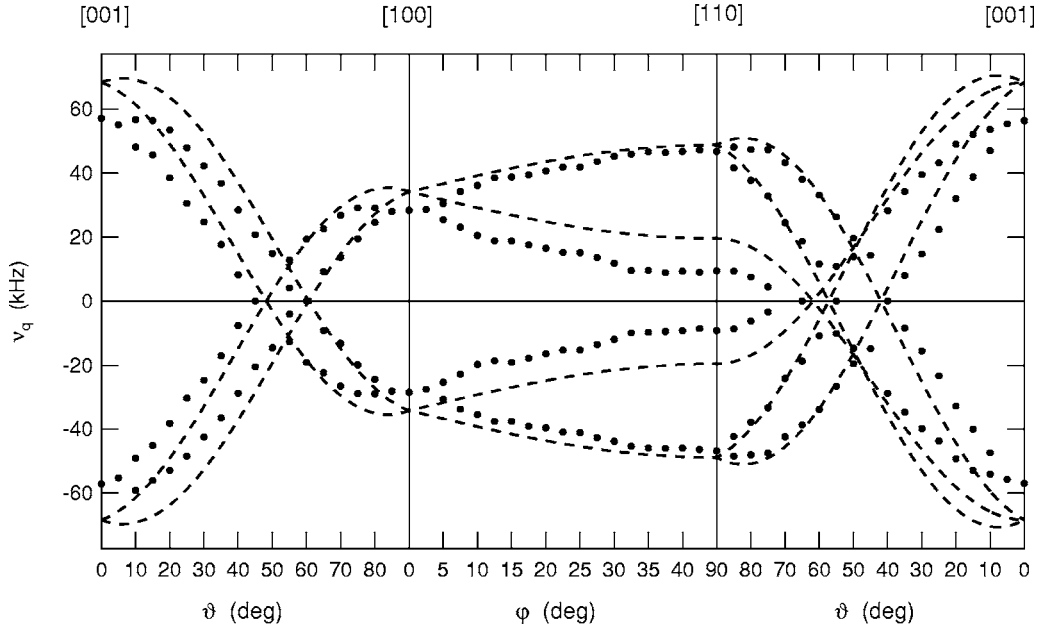
FIG. 4. Comparison of the resonance frequencies ν_q of the quadrupole satellites in the ^{7}Li NMR spectra of a LiAlO$_2$ single crystal (full circles) with the results of quantum chemical calculations (dashed lines). ϑ and φ denote the tilt angles of the magnetic field with respect to the main crystal axes which are given on the upper abscissa.

$$\vec{e}_{C,exp} = \begin{pmatrix} 0.701 \\ -0.701 \\ 0.133 \end{pmatrix}. \qquad (6)$$

From the quantum chemical calculations (see Sec. IV) we get the following EFG tensor:

$$V_{xx} = V_{yy} = 0.705 \text{ V/Å}^2,$$

$$V_{xy} = -0.302 \text{ V/Å}^2,$$

$$V_{xz} = -V_{yz} = 0.235 \text{ V/Å}^2. \qquad (7)$$

This yields the eigenvalues

$$V_{A,theo} = -1.456 \text{ V/Å}^2,$$

$$V_{B,theo} = 0.403 \text{ V/Å}^2,$$

$$V_{C,theo} = 1.052 \text{ V/Å}^2 \qquad (8)$$

and the corresponding eigenvectors

$$\vec{e}_{A,theo} = \begin{pmatrix} -0.094 \\ 0.094 \\ 0.991 \end{pmatrix}$$

$$\vec{e}_{B,theo} = \begin{pmatrix} 0.707 \\ 0.707 \\ 0 \end{pmatrix}$$

$$\vec{e}_{C,theo} = \begin{pmatrix} 0.701 \\ -0.701 \\ 0.133 \end{pmatrix}. \qquad (9)$$

Figure 4 shows the comparison of the experimental data with the results of the quantum chemical calculations. The input for these calculations was exclusively the crystallographic structure which was fully optimized at the same level of theory. In preliminary test calculations it was found that the calculated EFG tensor resonance frequencies do not change significantly when experimental lattice parameters are used instead. In both cases a good overall agreement is observed.

For orientations of the magnetic field between the [001] and the [110] direction of the crystallographic structure (right part in Figs. 3 and 4) the three-parameter fit and the quantum chemical calculations yield three different sets of quadrupole satellites. Experimentally these are visible only for large tilt angles ($70° < \vartheta < 90°$). For smaller tilt angles only two different sets of quadrupole satellites can be discriminated due to the width of the NMR lines (see also Fig. 2). This is the reason why the deviations between the experimental data and the fit curves are largest in this region.

VI. DISCUSSION

Comparing the results from the three-parameter fit to the experimental data with the quantum chemical calculations, we find good agreement for the eigenvalues and the eigenvectors. The largest deviation in the tensor components is 22% and no significant differences in the orientations of the eigenvectors are obtained. For the asymmetry parameter, defined as $\eta = (V_B - V_C)/V_A$ since $|V_B| < |V_C| < |V_A|$, we get $\eta_{exp} = 0.69 \pm 0.01$ and $\eta_{theo} = 0.446$. For the quadrupole coupling constant $C_q = e^2qQ/h$ where eq is the largest eigenvalue (by magnitude) of the EFG tensor, we get $C_{q,exp} = 115.1 \pm 0.6$ kHz and $C_{q,theo} = 141.1$ kHz. Experimentally the signs of the eigenvalues cannot be determined unambigu-

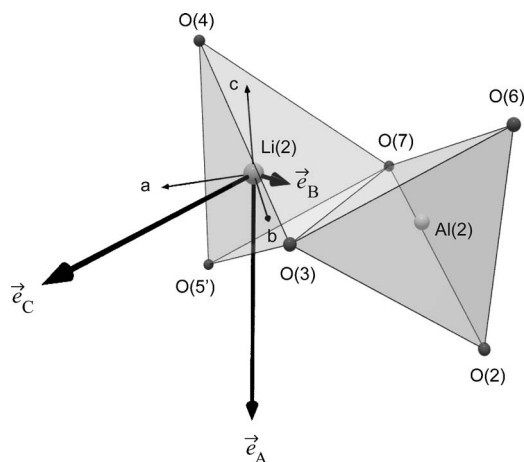FIG. 5. The elementary unit of the crystal structure of γ-LiAiO$_2$ consisting of a pair of LiO$_4$ and AlO$_4$ tetrahedra connected via a common edge. The bold arrows show the principal axes of the EFG tensor while their length is scaled to the corresponding eigenvalues. The thin arrows show the principal axes of the tetragonal crystal structure.

ously since the spectra are symmetric around the central resonance frequency ν_L. Only the comparison with the quantum chemical calculations shows that the choice of signs given in Eq. (5) is right.

The elementary unit of the crystal structure of γ-LiAlO$_2$ consists of a pair of LiO$_4$ and AlO$_4$ tetrahedra which are connected via a common edge, see Fig. 5. These units are connected via common oxygen corners to form the three-dimensional network depicted in Fig. 1. Figure 5 shows the

orientation of the EFG tensor's eigenvectors as arrows whose lengths are proportional to the corresponding eigenvalues. The eigenvector $\vec{e}_B$ is aligned exactly along the [110] direction, i.e., is pointing directly to the neighboring Al atom. $\vec{e}_A$ is slightly tilted from the z direction (by about 8°), following the tilting of the LiO$_4$ tetrahedron.

VII. CONCLUSION

We investigated the electric field gradient tensors in γ-LiAlO$_2$ at the Li sites by solid state NMR on a single crystalline sample. Three parameters were sufficient to fit the EFG tensor to our experimental data for all the four Li ions per unit cell simultaneously. By this we were able to determine the eigenvalues as well as the eigenvectors of the EFG tensor. These results will be used in further studies of the Li dynamics in γ-LiAlO$_2$, e.g., by temperature dependent NMR spectroscopy and conductivity measurements. From this the diffusion mechanism in this complex structure can be elucidated.

We find good agreement between the experimental results and theoretical calculations. This allows the identification of the Li position in cases where no experimental information is available. In summary, single crystalline γ-LiAlO$_2$ has proved to be a model system for the comprehensive and precise description of detailed experimental results on the local electronic structure by theoretical methods.

*Present address: Department of Chemistry, State University of New York at Stony Brook, 100 Nichols Rd., Stony Brook, NY 11794-3400, USA. Electronic address: sindris@ms.cc.sunysb.edu

†Electronic address: heitjans@pci.uni-hannover.de

‡Present address: Institut für Physikalische und Theoretische Chemie, Universität Bonn, Wegelerstraße 12, D-53115 Bonn, Germany.

[1] M. Marezio, Acta Crystallogr. **19**, 396 (1965).

[2] P. Waltereit, O. Brandt, and K. H. Ploog, Appl. Phys. Lett. **75**, 2029 (1999).

[3] H. Cao, B. Xia, Y. Zhang, and N. Xu, Solid State Ionics **176**, 911 (2005).

[4] M. A. K. L. Dissanayake, Ionics **10**, 221 (2004).

[5] J.-P. Jacobs, M. A. San Miguel, L. J. Alvarez, and P. B. Giral, J. Nucl. Mater. **232**, 131 (1996).

[6] D. Müller, W. Gessner, and G. Scheler, Polyhedron **2**, 1195 (1983).

[7] A. Abragam, *The Principles of Nuclear Magnetism* (Oxford University Press, Oxford, 1999).

[8] C. P. Slichter, *Principles of Magnetic Resonance* (Springer Verlag, Berlin, 1996).

[9] M. J. Duer, *Introduction to Solid-State NMR Spectroscopy* (Blackwell Publishing, Oxford, 2004).

[10] V. R. Saunders, R. Dovesi, C. Roetti, R. Orlando, C. M. Zicovich-Wilson, N. M. Harrison, K. Doll, B. Civalleri, I. Bush, Ph. D'Arco, M. Llunell, *CRYSTAL2003 User's Manual* (University of Torino, Torino, 2003).

[11] M. Catti, G. Valerio, R. Dovesi, and M. Causa, Phys. Rev. B **49**, 14179 (1994).

[12] M. I. McCarthy and N. M. Harrison, Phys. Rev. B **49**, 8574 (1994).

[13] T. Bredow, P. Heitjans, and M. Wilkening, Phys. Rev. B **70**, 115111 (2004).

[14] J. P. Perdew and Y. Wang, Phys. Rev. B **45**, 13244 (1992).

[15] H. J. Monkhorst, J. D. Pack, Phys. Rev. B **13**, 5188 (1976).

[16] P. Pyykkö, Mol. Phys. **99**, 1617 (2001).